ELSEVIER

Journal of Crystal Growth 232 (2001) 77–85

JOURNAL OF CRYSTAL GROWTH

www.elsevier.com/locate/jcrysgro

Dependence of nucleation kinetics and crystal morphology of a model protein system on ionic strength

V. Bhamidi[a], E. Skrzypczak-Jankun[b], C.A. Schall[a,*]

[a] *Department of Chemical & Environmental Engineering, The University of Toledo, 2801 W. Bancroft St., Toledo, OH 43606, USA*
[b] *Instrumentation Center, The University of Toledo, 2801 W. Bancroft St., Toledo, OH 43606, USA*

Abstract

Nucleation rate data for hen egg-white lysozyme crystallization were obtained using a particle counter. Tetragonal lysozyme crystals were expected to form at the temperature and solution conditions of these experiments: 4°C, pH 4.5 with 0.1 M sodium acetate buffer and 2–6% NaCl (w/v). The rates varied as expected, as smooth monotonic functions of supersaturation at 2%, 3% and 6% NaCl. However, at 5% NaCl, a great deal of scatter in the data was observed. At 2% and 3% NaCl, all the batches contained crystals with tetragonal morphology. At 6% NaCl, almost all of the vials contained the white powder with few or no tetragonal crystals. At 5% NaCl concentration, a mixture of tetragonal crystals and powder formed in varying proportions in all the vials as observed by visual inspection. The powdery material was examined using optical microscopy and was seen to consist of needles with regular structure and sharp, faceted edges. Powder diffraction data from these needles was inconsistent with experimental powder diffraction data from tetragonal lysozyme crystals. It is possible that at high salt and protein concentrations liquid-liquid separation occurred and yielded a crystal polymorph.

Keywords: A1. Nucleation; A2. Growth from solutions; B1. Lysozyme; B1. Proteins

1. Introduction

Structure determination of biomolecules is essential to an understanding of structure function relationships and to the rational development of strategies for disease treatment and pharmaceutical development. Many biomolecules of interest are proteins that can vary in size from 10 to 500 kDa. X-ray crystallography is the technique normally employed for structure determination of proteins larger than 20 kDa. In order to determine structure using X-ray crystallography, a crystal of suitable size must first be formed. Growth of protein crystals from solution also has application as a separation or purification process for protein products.

Crystallization can be modeled as two distinct processes consisting of nucleation and crystal growth. Nuclei are clusters of solute molecules of sufficient size such that growth and dissolution are equally likely events. Addition of solute molecules to these nuclei results in an aggregate of molecules that will grow in size to form crystals.

Supersaturation, the concentration of solute in solution above equilibrium solubility, provides a driving force for both nucleation and crystal growth. The supersaturation required for nucleation is much higher than that required for crystal growth. Lowering temperature, increasing ionic

*Corresponding author. Tel.: +1-419-530-8097; fax: +1-419-530-8086.

E-mail address: cschall@eng.utoledo.edu (C.A. Schall).

0022-0248/01/$ - see front matter
PII: S0022-0248(01)01143-5

strength, adjusting pH or simply increasing protein concentration can often increase supersaturation and influence nucleation [1].

Many light scattering studies have addressed the behavior of protein solutions under crystallizing conditions in terms of aggregate formation and nucleation induction time [2–4]. These studies relate solution conditions to the formation of nuclei and the time required for the first appearance of these nuclei, the induction time.

At high protein concentration or low temperatures, liquid–liquid phase separation has also been found to occur in several protein systems [5,6]. In a protein-rich phase, crystal nucleation rates are expected to be accelerated [7]. In a computer simulation study, it was found that the presence of a metastable fluid-fluid critical point drastically changes the pathway for the formation of a critical nucleus and the large density fluctuations near the critical point increase the nucleation rate [8]. Haas and Drenth discuss the nucleation mechanisms in the liquid-liquid phase separation zone [9] and attempt a theoretical explanation for enhanced nucleation rates. Liquid–liquid spinodal decomposition followed by nucleation was proposed by Georgalis et al. [10]. They also observed the formation of 'sea urchin' lysozyme crystallites from coalescing domains of the phases.

The structure or arrangement of the protein in the solid phase is influenced by many of the same factors that influence nucleation: protein concentration, pH, precipitant type and concentration, and pH [11]. Structurally dissimilar solid phases are referred to as polymorphs. In general, polymorphs differ in solubility. If the solid product is a pharmaceutical, polymorphs can differ in dissolution rate and therefore bioavailablity [12]. At very high levels of supersaturation unstable polymorphs can form with subsequent solid–solid transitions to a more stable solid state.

We measured the nucleation rate of hen egg-white lysozyme crystals at varying protein and precipitant concentrations. The precipitant used in these studies was NaCl. Under conditions of high salt and high protein concentrations, morphology of the resulting solid phase differed from the expected tetragonal crystal morphology.

2. Materials and methods

2.1. Solutions

Hen egg-white lysozyme (Seikagaku) was dissolved in 0.1 M sodium acetate buffer at a pH of 4.5. The buffer was exchanged three times with a pressure concentrator (Millipore or Sartorius) using 10000 or 8000 MWCO membranes. The concentrated protein stock was filtered through 0.2 μm syringe filters (Corning). The concentration of protein in solution was determined by measuring the absorbance at 280 nm using an extinction coefficient of 2.64 absorbance units per 1 mg/ml solution and a 1 cm light path [13]. Sodium chloride solutions were prepared by dissolving the required amount of NaCl in sodium acetate buffer. The protein concentration was adjusted by adding buffer to the protein stock. Both the protein solution and the salt solution were precooled at 4°C for at least 1 h before they were mixed. The final crystallizing batch solution was prepared by mixing 4 ml of protein solution and 4 ml of salt solution for a final NaCl concentration of 2%, 3%, 5% or 6% (w/v). The mixture was filtered into a clean 20 ml scintillation vial through a 0.1 μm syringe filter (Millipore). The vial was then placed on the particle counter stage.

The protein concentration range studied was varied with the salt concentration. Defining supersaturation as the ratio of protein concentration to tetragonal hen egg-white lysozyme solubility (C/C^*), the range of supersaturation studied was from about 10 to 20 at 2%, 3% and 6% NaCl, and from 10 to 35 at 5% NaCl. This corresponds to the protein concentration ranges of approximately 27–60, 10–19, 4–15 and 3–7 mg/ml for 2%, 3%, 5% and 6% NaCl, respectively. Many of the experiments were performed in triplicate, with as many as five replicates in some cases at 5% NaCl.

2.2. Particle counting

A particle counter, PC2000, from Spectrex Corporation was used to obtain the number density of crystals in the crystallizing solution with respect to time. This instrument uses the principle of near angle light scatter to detect

particles in the solution. A revolving laser beam passes through the walls of the vial and illuminates a fixed volume of liquid in the sensing zone. As the laser beam moves across a particle suspended in the sensing zone, light from the beam will be scattered. Much of this scattered light is in the near-forward direction and is collected by the optical system of the photodetector assembly. The flash of light striking the photodetector will cause an electrical pulse in the preamplifier connected to the photodetector. The number of pulses indicates the number of particles present and the amplitude of the pulse is used to size the particle.

The counter can be programmed to obtain the number density of particles in the solution over time. The counter was calibrated with Clintex particle standards of size 10.35 μm, obtained from Pacific Scientific. This standard contains 1000 particles per ml, and various dilutions of the standard were employed in calibrating the instrument. The change in the number density of particles with time, immediately after mixing the protein and the salt solutions, yields the rate of nucleation. The particle counter was placed in an incubator for precise temperature control ($\pm 0.1^{\circ}$C) and data were collected at 4°C.

After collection of rate data, a number of vials were kept at 4°C for about six months, and the protein concentration in the supernatant solutions was measured to obtain solubility information.

2.3. Powder diffraction

Crystals with needle or 'sea urchin' morphology were formed in addition to the expected tetragonal form of lysozyme. Therefore, both types of crystals were examined using X-ray powder diffraction to obtain information about possible differences in the solid structure. The crystals with needle morphology were too small for single crystal X-ray analysis. The size of a single needle crystal did not exceed 50 μm in the longest dimension and 5 μm in the shortest dimension. These crystals were not powdered or ground further. Needles were transferred into a 1 mm glass capillary tube and were stabilized by a saturated lysozyme solution with the same solution conditions from which the needles were obtained. Tetragonal crystals were crushed in an eppendorf tube using a spatula. This powder was then transferred into a 1 mm glass capillary tube and was stabilized using the same solution as described above. A solid mixture of sodium acetate and sodium chloride in the ratio found in the crystallizing solution was prepared by grinding these salts using a mortar and pestle and placed in a capillary tube. The capillary tubes were sealed with wax. Diffraction data were collected using a Rigaku R-axis IV image plate detector with a 50 kV, 100 mA rotating copper anode and focusing mirrors, using an oscillation of 240° and 30 min exposure time at a 100 mm crystal-to-detector distance.

3. Results

The number of particles formed in the sensing zone of the particle counter was tabulated at small time intervals. Only particles greater than 0.5 μm in size were detectable. Stable nuclei are assumed to grow into crystals that can be counted. The rate of particle formation is then determined from the slope of a plot of number density versus time as shown in Fig. 1. At short run times the supersaturation of protein changes insignificantly as calculated from a mass balance of particle density and size and initial protein mass in solution. Using this method, the rate of particle formation, or nucleation rate, can be determined at the initial solution conditions.

Tetragonal lysozyme crystals were expected to form at the temperature and solution conditions of these experiments; 4°C, pH 4.5 with 0.1 M sodium acetate buffer and 2–6% NaCl (w/v). Fig. 2 summarizes the nucleation rate data at 3%, 5% and 6% NaCl as a function of protein concentration. The lines drawn are exponential fits to the data. The rates vary as expected, as smooth monotonic functions of supersaturation at 2%, 3% and 6% NaCl. (Data are not shown for 2% NaCl in Fig. 2 for clearer presentation of the data.) However, at 5% NaCl, a great deal of scatter in the data was observed. At the conclusion of the experiments, the crystallizing batches were examined and some were found to contain a white powdery material along with regular tetragonal crystals. At 2% and 3% NaCl, all the batches

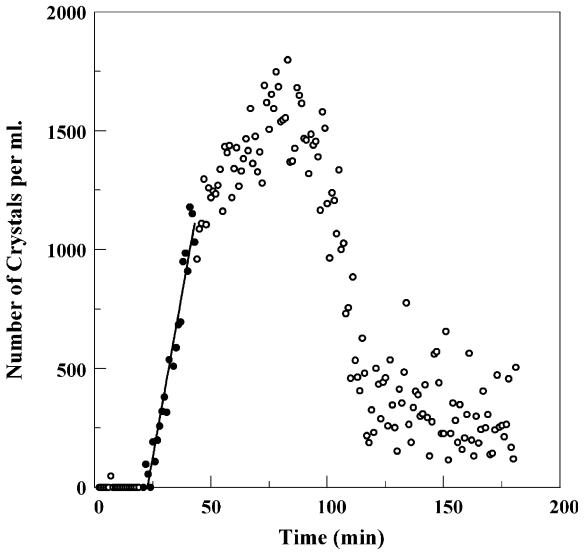

Fig. 1. Typical nucleation rate data set. Number density of particles is plotted against time. The slope during the initial time period gives the nucleation rate. At very long run times the number density of particles drops due to settling of large crystals out of the instrument's sensing zone. Because crystals must first grow to a detectable size after nucleation has occurred, particles may not be detected at early times.

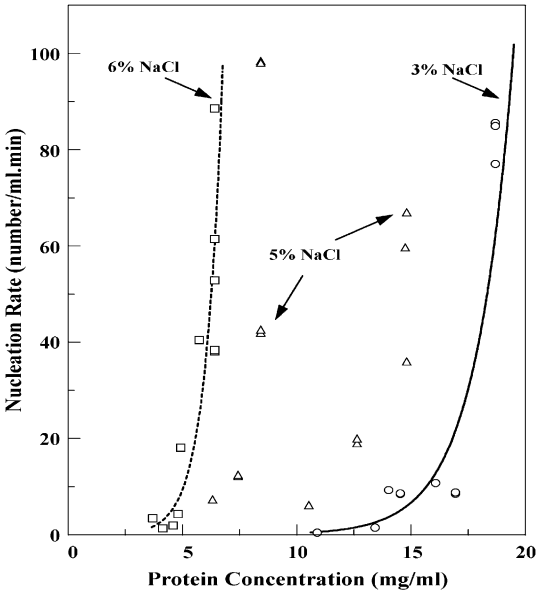

Fig. 2. Nucleation rates at various NaCl concentrations plotted against protein concentration. At 3% and 6% NaCl concentrations, the rate data appear to vary smoothly with protein concentration, whereas at 5% NaCl there is much scatter in the data.

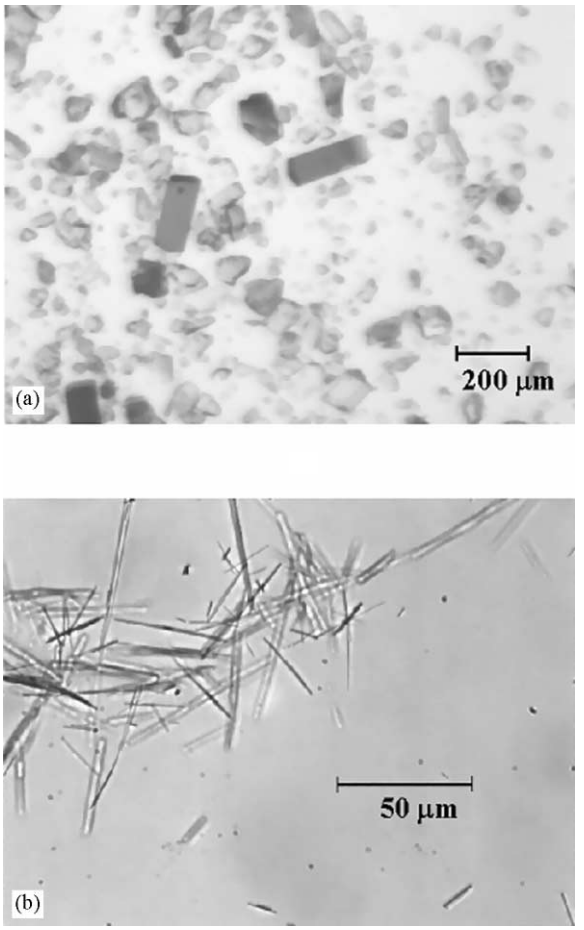

Fig. 3. (a) Crystals formed in vials with 2% and 3% NaCl exhibited the common tetragonal crystal morphology as viewed with an optical microscope at a magnification of 40 ×. (b) The powdery solids that formed frequently at 5% and 6% NaCl had a 'sea urchin' morphology at lower magnification, but clearly had faceted edges when viewed at higher magnification, 400 ×, as shown in.

contained crystals with tetragonal morphology. At 6% NaCl, almost all of the vials contained the white powder with few or no tetragonal crystals. A mixture of tetragonal crystals with a small amount of powder formed at low protein concentrations (below 5 mg/ml) in 6% NaCl. At 5% NaCl concentration, a mixture of tetragonal crystals and powder formed in varying proportions in all the vials as observed by visual inspection. The powdery material was examined using optical microscopy (Fig. 3). At low magnification the

material appeared as clumps with 'sea-urchin' morphology reported by others in crystallizing lysozyme [14–16]. However, under high magnification, the powdery material was seen to consist of needles with regular structure and sharp, faceted edges, approximately 5–50 μm in the longest dimension.

Although others have reported the presence of needles (as clumps or 'sea urchins') in crystallizing lysozyme, this solid phase is poorly characterized. It was thought that a measurement of solubility might offer information about the structure and stability of these needles. The concentration of protein in the supernatants of batches that were incubated at 4°C for about six months was measured. The concentration obtained from the vials containing 2% NaCl was 3.001 ± 0.091 mg/ml. This was in good agreement with a calculated solubility value of tetragonal lysozyme crystals of 3.022 mg/ml [17], suggesting that the batches were near equilibrium. The concentration measured at 5% NaCl was 0.464 mg/ml in a vial that contained predominantly needles with a small amount of tetragonal crystals. Two vials of tetragonal crystals with 5% NaCl had supernatant concentrations of 0.402 and 0.397 mg/ml, which are less than a calculated tetragonal lysozyme crystal solubility value of 0.532 mg/ml [17]. The supernatant concentration in the vials containing predominantly tetragonal crystals in 6% NaCl was 0.320 ± 0.016 mg/ml, again lower than a calculated solubility value of 0.405 mg/ml. The supernatant concentration from a vial with predominantly needles at 6% NaCl was 0.486 mg/ml, which is significantly greater than that from the vials with tetragonal crystals. It should be noted that the regression coefficients reported in the above reference [17] to estimate tetragonal lysozyme crystal solubility also have some degree of uncertainty, the largest margin being at 5% NaCl with a reported average deviation of 13.8%. In general, supernatant concentrations from vials containing needles appear to be greater than those from vials with tetragonal crystals. An increasing number of tetragonal crystals appeared in the vials with needles as incubation time progressed.

Von Dreele has recently performed a Rietveld refinement of sperm whale metmyoglobin by combining high-resolution X-ray powder diffraction data obtained using a synchrotron source with stereochemical restraints [18]. To obtain information on the crystallinity and structure of the needles formed at high salt and protein concentration we performed powder diffraction studies (since single crystal X-ray diffraction of the needle crystals was not possible due to their small size). A powder diffractometer with a Cu X-ray tube operating at 2 kW was not suitable for our needle sample and so an imaging plate detector with a 5 kW X-ray source was used as described in the Materials and Methods section. For comparison, powder diffraction data were acquired for the buffer-salt mixture (sodium acetate and sodium chloride) and tetragonal lysozyme crystals. The needle powder diffraction data yielded a pattern of well-formed concentric rings of variable intensity, confirming that the needles are crystalline (Fig. 4). In Fig. 5, intensity as a function of scattering angle, 2θ, is shown for the needles, tetragonal crystals and buffer salts. Differences in the diffraction patterns are apparent. When comparing the needle and tetragonal crystal data, there are shifts

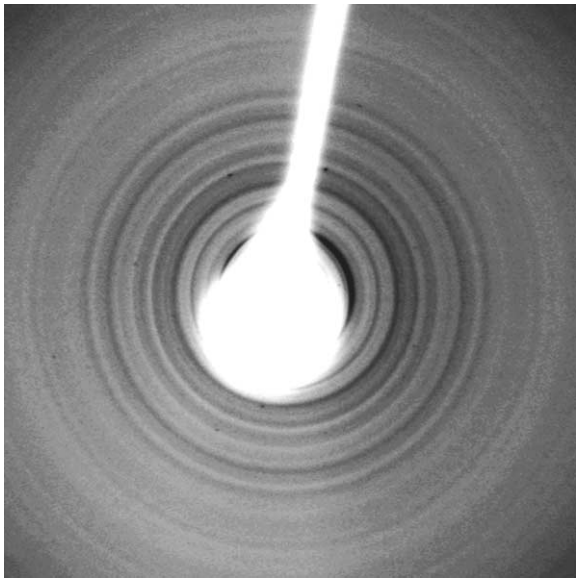

Fig. 4. The powder pattern of the needle crystals formed in samples with high salt content (5% NaCl and greater) has distinct rings, indicating that the needles are crystalline.

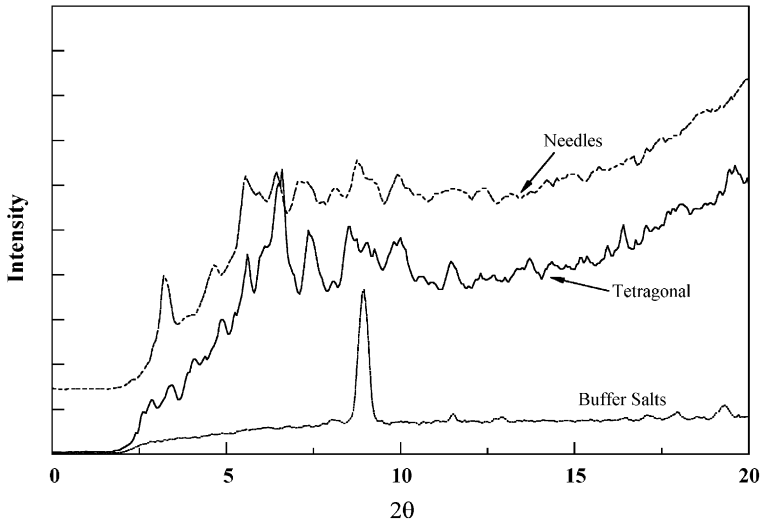

Fig. 5. Intensity versus 2θ for needle crystals, a powdered tetragonal crystal sample and a sodium acetate/sodium chloride buffer mixture.

of some of the more intense peaks. Most notably, an intense peak in the needle pattern, at about 3 degrees, is missing in the tetragonal pattern. The pattern for the buffer salts is quite different, with peaks well removed from most of the peaks for both the needle and the tetragonal crystals.

To compare the powder patterns rationally, a tetragonal powder pattern of hen egg-white lysozyme was simulated using the structure factors and coordinates taken from file 193L in the Protein Data Bank [19] and 'xpro' and 'xpow' programs from SHELXTL, Unix ver. 5.1, (Bruker AXS). Using xpow, intensity versus 2θ was plotted and the nine most intense peaks in the tetragonal form of lysozyme were identified and labeled A–I, with A being the most intense peak (Fig. 6). The nine peaks were found to be clearly visible in the powder pattern of the tetragonal crystals that was acquired (Fig. 6). The simulated tetragonal powder pattern was then compared to the needle powder diffraction data. Some of the major tetragonal peaks are missing in the needle powder pattern, particularly C. We also see a shift in relative intensities in some major peaks. For example, the relative intensities of A and B differ in the needle and tetragonal powder diffraction pattern. There is also a fairly intense peak at low angle, at about 3 degrees, in the needle powder

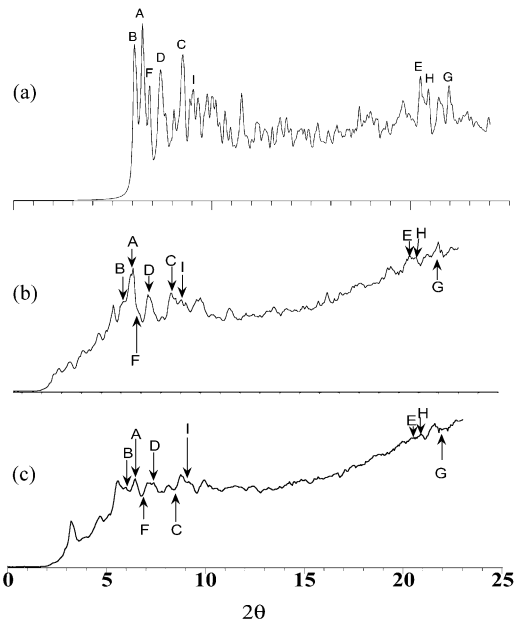

Fig. 6. Intensity versus 2θ for (a) a simulated powder pattern for tetragonal crystals, (b) powdered tetragonal crystals and (c) needle crystals. The intense peaks in the simulated powdered pattern are ranked from A to I with A being the most intense peak. The locations of these peaks are indicated on the tetragonal and needle powder diffraction data. There is a good match between the simulated tetragonal powder pattern and the experimental tetragonal data. The match between the simulated pattern and the needle data is poor.

pattern that is not present in the tetragonal powder pattern. Our needle crystal powder diffraction pattern is inconsistent with the tetragonal powder pattern.

To explore the possibility of the needles being one of the known morphologies of lysozyme crystals, powder patterns of monoclinic, orthorhombic and triclinic lysozyme crystals were simulated and these were compared to the needle pattern. The structure factors and coordinates were taken from files 1LKR (monoclinic), 1AKI (orthorhombic) and 1LKS (triclinic) of the Protein Data Bank [19] to generate the simulated patterns. A definite match between these simulated powder patterns and the needle pattern could not be perceived. Low angle intensity data may be helpful in determining the unit cell parameters of the needles, but these data were masked in our experiments by the beam stopper.

4. Discussion

In the incubated batches with 2% and 3% NaCl, lysozyme crystals exhibited the expected tetragonal morphology, whereas at 6% NaCl, crystals exhibited predominantly needle-like morphology in most batches. The nucleation rate data obtained at these NaCl concentrations were smooth with respect to protein concentration. At 5% NaCl, a mixture of tetragonal and needle morphologies could be seen in many batches. The large scatter in the rate data obtained with 5% NaCl could be separated into two groups as shown in Fig. 7. These curves may correspond to the formation of either predominantly needle or predominantly tetragonal crystals. In a previous study a similar split in nucleation rate data was observed at 4% NaCl that was attributed to liquid–liquid phase separation [16].

It is known that liquid–liquid phase separation occurs in protein solutions. Muschol and Rosenberger experimentally determined the liquid–liquid coexistence region, or cloud points, for highly concentrated solutions of hen egg-white lysozyme in 3%, 5% and 7% NaCl at our buffer conditions [15]. Using a correlation predicted by group normalization theory, they calculated cloud point

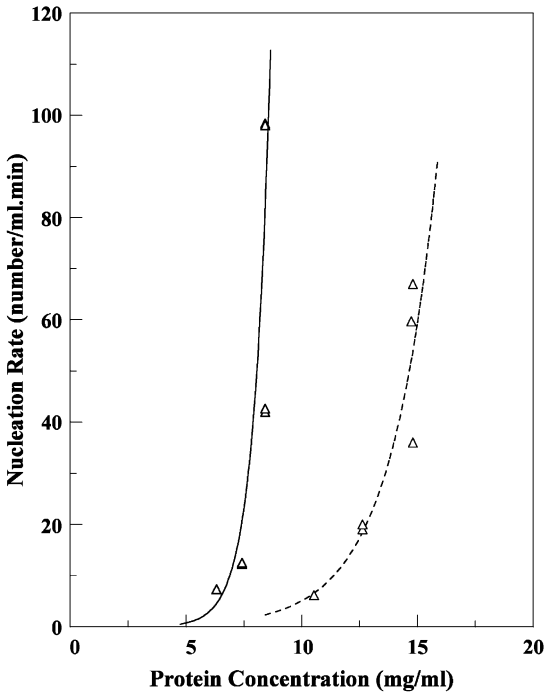

Fig. 7. The nucleation rate data at 5% NaCl is broken into two groups. At lower protein concentrations, tetragonal crystals formed and data were fit to an exponential function (solid line). At protein concentrations greater than 8.5 mg/ml data were grouped and fit to a second exponential function (dashed line). In this second data group, vials contained both needle and tetragonal crystals.

temperatures as a function of protein concentration. Darcy and Wiencek compared these predicted cloud point temperatures extrapolated to low protein concentrations for 5% and 7% NaCl solutions to their measured cloud point temperatures in less concentrated lysozyme solutions [20]. They found that the extrapolated cloud point predictions overestimated the cloud point temperatures at the lower protein concentrations used in their studies. The protein concentrations in our nucleation studies were in the range of values examined by Darcy and Wiencek. The measured cloud point temperatures are well below our solution temperature of 4°C except at the highest protein concentration used in our studies at 5% NaCl (15 mg/ml). However, the cloud point temperature as predicted by Muschol and Rosenberger is above our solution temperature. In

lysozyme solutions, increasing salt concentration increases the cloud point temperatures [15,20] and decreases the solubility. This means that the solid-liquid coexistence region approaches the liquid–liquid phase separation region as salt content is increased. The lower salt concentrations, 2% and 3% NaCl, and protein concentrations used in these studies were well away from the liquid–liquid coexistence region even as conservatively predicted by Muschol. Only tetragonal crystals formed at these salt concentrations. At 6% NaCl, our solution conditions may be below the cloud point and the crystals exhibited predominantly needle-like morphology. At 5% NaCl we may have a mixture of conditions where at lower protein concentrations we are nucleating crystals above the cloud point and at higher protein concentrations we are nucleating crystals below the cloud point. At a protein concentration of $8.4\,\mathrm{mg\,ml^{-1}}$ at 5% NaCl five repeats were performed. In three of these repeats tetragonal crystals formed at a nucleation rate of $98.3 \pm 0.2\,\mathrm{ml^{-1}\,min^{-1}}$. In the samples that appear to form predominantly needles with a small amount of tetragonal crystals, the apparent nucleation rates were 42.0 and $42.6\,\mathrm{ml^{-1}\,min^{-1}}$.

If a liquid–liquid phase separation occurs, it is expected that a protein rich and protein lean phase would form. According to Muschol and Rosenberger the protein rich phase can contain up to $400–500\,\mathrm{mg\,ml^{-1}}$ of protein. It is expected that nucleation rates would be very high at these concentrations. However, a simple mass balance based on the above estimated concentration of the protein rich phase shows that the volume of protein rich phase transiently formed is very small compared to the total solution volume. If liquid–liquid phase separation occurs in the vicinity of $8.5\,\mathrm{mg\,ml^{-1}}$ with 5% NaCl, an infinitesimally small volume of protein rich phase would form at this concentration. Even if nucleation rates are very high in the protein rich phase, the apparent nucleation rate drops when averaged over the total solution volume. The resulting protein-rich phase may produce an unstable crystal polymorph with the observed needle morphology. These crystals may then act as seeds for further nucleation.

The batches of crystals were incubated over several months and tetragonal crystals appeared in the batches where initially only needles were visible directly after a nucleation rate experiment. Additionally, the supernatant concentration in aged samples with predominantly needle crystals was consistently higher than that of samples with tetragonal crystals at the same salt concentrations. These observations are consistent with the assumption that the needle crystals are an unstable polymorph of crystalline lysozyme that slowly converts to the tetragonal form. It is possible that a highly protein-rich phase may be affecting the nucleation process at high salt concentration, giving rise to an unstable polymorph.

Polymorphs can vary in stability. As an example, the amorphous form of insulin was observed to be more stable than the crystalline form, contrary to the expectations [21]. As mentioned previously, polymorphism in pharmaceutical products may affect bioavailability and effectiveness. For structure determination, one needs to have stable crystals. Nucleating a protein crystal can be a challenging task in some cases. Since the liquid–liquid phase separation region offers localized enhancement in nucleation rates, it might appear that an attempt to crystallize a protein at those conditions is a good approach. However, the possibility of forming an unstable polymorph at those conditions can undermine the efficacy of that strategy.

Acknowledgements

This work was funded by a National Institutes of Health grant GM55933-02 and NASA grant NAG8-1578. The authors would like to thank Sasidhar Varanasi for helpful discussions. The Instrumentation Center in the College of Arts & Sciences at the University of Toledo is acknowledged for providing support and services for the X-ray diffraction experiments.

References

[1] R.A. Judge, R.S. Jacobs, T. Frazier, E.H. Snell, M.L. Pusey, Biophys. J. 77 (1999) 1585.
[2] A.J. Malkin, A. McPherson, Acta Crystallogr. D 50 (1995) 385.

[3] B. Biscans, C. Laguerie, J. Phys. D 26 (1993) B118.
[4] M. Skouri, B. Lorber, R. Giege, J. Munch, J. Candau, J. Crystal Growth 152 (1995) 209.
[5] C. Ishimoto, T. Tanaka, Phys. Rev. Lett. 39 (1977) 474.
[6] V.G. Taratuta, A. Holschbach, G.M. Thurston, D. Blankschtein, G.B. Benedek, J. Phys. Chem. 94 (1990) 2140.
[7] P. Rein ten Wolde, D. Frenkel, Sci. 277 (1997) 1975.
[8] P. Rein ten Wolde, D. Frenkel, Theor. Chem. Accounts 101 (1999) 205.
[9] C. Haas, J. Drenth, J. Chem. Phys. B 104 (2) (2000) 368.
[10] Y. Georgalis, P. Umbach, D.M. Soumpasis, W. Saenger, J. Am. Chem. Soc. 120 (1998) 5539.
[11] L.F. Kuyper, C.W. Carter, J. Crystal Growth 168 (1996) 155.
[12] E. Garcia, S. Veesler, R. Boistelle, C. Hoff, J. Crystal Growth 198/199 (1999) 1360.
[13] A.J. Sophianopoulos, C.K. Rhodes, D.W. Holcomb, K.E. VanHolde, J. Biol. Chem. 237 (1962) 1107.
[14] F.L. Ewing, E.L. Forsythe, M. van der Woerd, M.L. Pusey, J. Crystal Growth 160 (1996) 389.
[15] M. Muschol, F. Rosenberger, J. Chem. Phys. 107 (6) (1997) 1953.
[16] O. Galkin, P.G. Vekilov, J. Am. Chem. Soc. 122 (1) (2000) 156.
[17] E. Cacioppo, M.L. Pusey, J. Crystal Growth 114 (1991) 286.
[18] R.B. Von Dreele, J. Appl. Crystallogr. 32 (1999) 1084.
[19] H.M. Berman, J. Westbrook, Z. Feng, G. Gilliland et al., Nucl. Acids Res. 28 (2000) 235.
[20] P.A. Darcy, J.M. Wiencek, J. Crystal Growth 196 (1999) 243.
[21] M.J. Pikal, D.R. Rigsbee, Pharmaceutical Res. 14 (10) (1997) 1379.